

PAPER • OPEN ACCESS

## Patterns and trends of heat and wildfire smoke indicators across rural–urban and social vulnerability gradients in Idaho

To cite this article: Seyd Teymoor Seydi *et al* 2025 *Environ. Res.: Health* **3** 015009

View the [article online](#) for updates and enhancements.

You may also like

- [A systematic review of urban green and blue spaces and cognitive function including discussion of mechanistic pathways](#)  
Sophie Glover, Claire L Cleland, Mike Trott et al.
- [Comparing indoor and outdoor temperature and air pollution at an urban cooling center: a multiyear case study](#)  
Daniel L Mendoza, Erik T Crosman, Corbin Anderson et al.
- [Causally inferred evidence of the impact of green and blue spaces \(GBS\) on maternal and neonatal health: a systematic review and meta-analysis](#)  
Rukun K S Khalaf, Selin Akaraci, Faye D Baldwin et al.



**UNITED THROUGH SCIENCE & TECHNOLOGY**

 **The Electrochemical Society**  
Advancing solid state & electrochemical science & technology

**248th  
ECS Meeting**  
Chicago, IL  
October 12-16, 2025  
*Hilton Chicago*

**Science +  
Technology +  
YOU!**

**SUBMIT  
ABSTRACTS by  
March 28, 2025**

**SUBMIT NOW**

# ENVIRONMENTAL RESEARCH HEALTH



## PAPER

# Patterns and trends of heat and wildfire smoke indicators across rural–urban and social vulnerability gradients in Idaho

### OPEN ACCESS

RECEIVED  
23 July 2024

REVISED  
19 December 2024




ACCEPTED FOR PUBLICATION  
8 January 2025

PUBLISHED  
17 January 2025

Original content from this work may be used under the terms of the [Creative Commons Attribution 4.0 licence](#).

Any further distribution of this work must maintain attribution to the author(s) and the title of the work, journal citation and DOI.



Seyd Teymoor Seydi<sup>1</sup> , Jennifer Pierce<sup>2</sup>, John T Abatzoglou<sup>3</sup> , Anna Radin<sup>4</sup>, Ethan Sims<sup>4</sup>, Hilary Flint<sup>4</sup>, Stephanie Wicks<sup>4</sup>, Eric Henderson<sup>5</sup>, Bhaskar Chittoori<sup>1</sup> and Mojtaba Sadegh<sup>1,6,\*</sup> 

<sup>1</sup> Department of Civil Engineering, Boise State University, Boise, ID 83725, United States of America

<sup>2</sup> Department of Geosciences, Boise State University, Boise, ID 83725, United States of America

<sup>3</sup> Management of Complex Systems Department, University of California, Merced, CA 95343, United States of America

<sup>4</sup> St Luke's Health System, Boise, ID 83725, United States of America

<sup>5</sup> Department of Computer Science, Boise State University, Boise, ID 83725, United States of America

<sup>6</sup> United Nations University Institute for Water, Environment and Health (UNU-INWEH), Hamilton, ON, Canada

\* Author to whom any correspondence should be addressed.

E-mail: [mojtabasadeqh@boisestate.edu](mailto:mojtabasadeqh@boisestate.edu)

**Keywords:** heatwave, wildfire smoke, exposure, social vulnerability, urban vs rural

Supplementary material for this article is available [online](#)

## Abstract

Climate change poses a grave threat to human health with disparate impacts across society. While populations with high social vulnerability generally bear a larger burden of exposure to and impact from environmental hazards; such patterns and trends are less explored at the confluence of social vulnerability and rural–urban gradients. We show that in rural regions in Idaho, low vulnerability populations had both the highest long-term average and the highest increase rate of exposure to heatwaves from 2002–2020, coincident with a higher population density in low—as compared to high—vulnerability rural census tracts. In urban areas, however, high vulnerability populations accounted for the highest long-term average and increase rate of heatwave exposure; they also accounted for highest population density. Contrary to regional warming trends, population-weighted maximum summer land surface temperature (LST-Max) showed a negative trend across Idaho in the past two decades coincident with increasing neighborhood greenness. Our results show that increasing population density in southern Idaho with a Mediterranean climate and hot summers is correlated with increasing greenness—associated with development of barren land and growing trees planted in former developments—and declining LST-Max. Furthermore, we show that while ambient air quality in the past two decades improved in southern Idaho—consistent with national trends—it worsened in northern Idaho. Wildfire smoke concentrations also increased across Idaho, with pronounced trends in northern Idaho. Our findings indicate that while climatic extremes continue to increasingly threaten human lives, nature-based solutions—such as neighborhood greening, where allowed by environmental and social factors—can mitigate some of the adverse impacts of climate change.

## 1. Introduction

Climatic changes have increasingly impacted human lives and livelihood across the globe in recent decades [1]. The western US, for example, faces a variety of climate-related extremes, including drought, heatwaves, wildfires, and wildfire smoke [2]. Specifically, heatwaves' intensity, frequency, magnitude, and geographical extent of impact have been increasing in recent decades [3], resulting in a multitude of human impacts ranging from agricultural failure [4, 5] and electric grid disruptions [6] to increased human morbidity and mortality [7]. Heatwaves are indeed one of the deadliest natural hazards, which claimed more than 166 000

deaths globally (likely an underestimation) between 1998 and 2017 [8]. Wildfires also increasingly threaten humans and infrastructure across the western US [9]. While the immediate threat of wildfires to human lives is grave, smoke spreads wildfire impacts to millions of people hundreds-to-thousands of kilometers away from the burned areas and extend the impacts for days-to-weeks [10].

Climate-related extremes differentially impact various strata of population, with a disproportionately larger burden on the poor, elderly, and other socially vulnerable individuals and communities [11]. A recent study, for example, showed that the lowest income quartile population of the world have already observed 30% larger heatwave exposure than the highest income quartile [12]. Moreover, the compounding impacts of intensifying heatwaves, limited adaptation capacity and higher population growth rates of low-income countries are expected to further widen this gap in vulnerability and inequality by the end of the century [12, 13]. Similar trends and patterns are observed in the exposure of socially vulnerable populations and communities to various extremes across the US [14–17]. Social vulnerability refers to the susceptibility of individuals, communities, and societies to negative impacts from hazards [18].

Adapting to climate change is crucial for safeguarding communities, economies, and ecosystems against increasingly severe impacts of climate extremes [19, 20]. Historical and contemporary social, economic, and institutional factors, however, influence the ability of communities to prepare for, respond to, and recover from disasters [21]. Studies have endeavored to represent these factors in proxies such as social vulnerability indices, and summarize them into a readily available metric. Various studies have used these indices to investigate the differential impacts of environmental hazards and disasters on communities [22]. Social vulnerability indices, however, may not entirely represent challenges faced by urban versus rural populations with respect to climatic extremes [23]. While urban populations face pronounced extremes due to biophysical traits of built-up areas—e.g. decreased green areas and diminished evaporative cooling, heat entrapment and urban heat islands (UHIs)—rural areas also face unique challenges due to their elevated dependence on natural resources, geographic and demographic challenges in preparing for and responding to extremes, and challenges associated with infrastructure availability and access—including transportation, health care and emergency response systems [24]. Climate impact assessments should factor in all these considerations to accurately inform community resilience efforts [25].

Here we focus on Idaho in the northwest US which has the fastest growing population in the nation [26], and is one of the most rural states with 80% of counties classified as rural [27]. The U.S. Census Bureau defines a rural area as any geographic area not categorized as urban, meaning rural areas consist of open land and communities with fewer than 5000 residents and less than 2000 housing units. Idaho accounted for 14% of all burned areas in the contiguous US from 2000 to 2019—second only to California [28]. The continental and xeric climate of Idaho drives drought, heatwaves and other climate extremes, with maximum daily temperatures in summer in southern Idaho frequently exceeding 37.8 °C (100) in summer. In addition, easterly winds frequently blanket Idaho in smoke from wildfires in western states [29]. It is important to note, however, that Idaho also benefits from unique availability of natural resources; for example, ranking first in water withdrawal per capita in the US [30]. Given these unique, and understudied, social and environmental conditions in Idaho, we leveraged meteorological data, satellite data and products, and census and population data, along with geospatial and statistical methods to answer:

1. What are the trends of heat and wildfire smoke indicators, and associated social and environmental factors, across Idaho in recent decades?
2. How is the ‘equity-scape’ of climate extremes across social vulnerability and rural–urban gradients over Idaho?

## 2. Materials and methods

### 2.1. Study area

Our study domain is the state of Idaho (figure 1(a)), with distinct environmental and social gradients. Idaho’s vast expanse of approximately 216 430 sq-km stretches across the northwest US. Its unique geography is characterized by diverse landscapes ranging from rugged mountains to vast plains, and its latitudinal and elevational features create diverse climates [26]. Idaho’s population nearly doubled from 1990 to 2022, with most of its population living in a limited number of urban centers in the south (figures 1(b) and (c)). Due to their distinct features, we analyze northern and southern Idaho separately (figure 1(a)), and further focus on urban vs rural populations in each region. Table 1 lists the ecoclimatic and population differences between

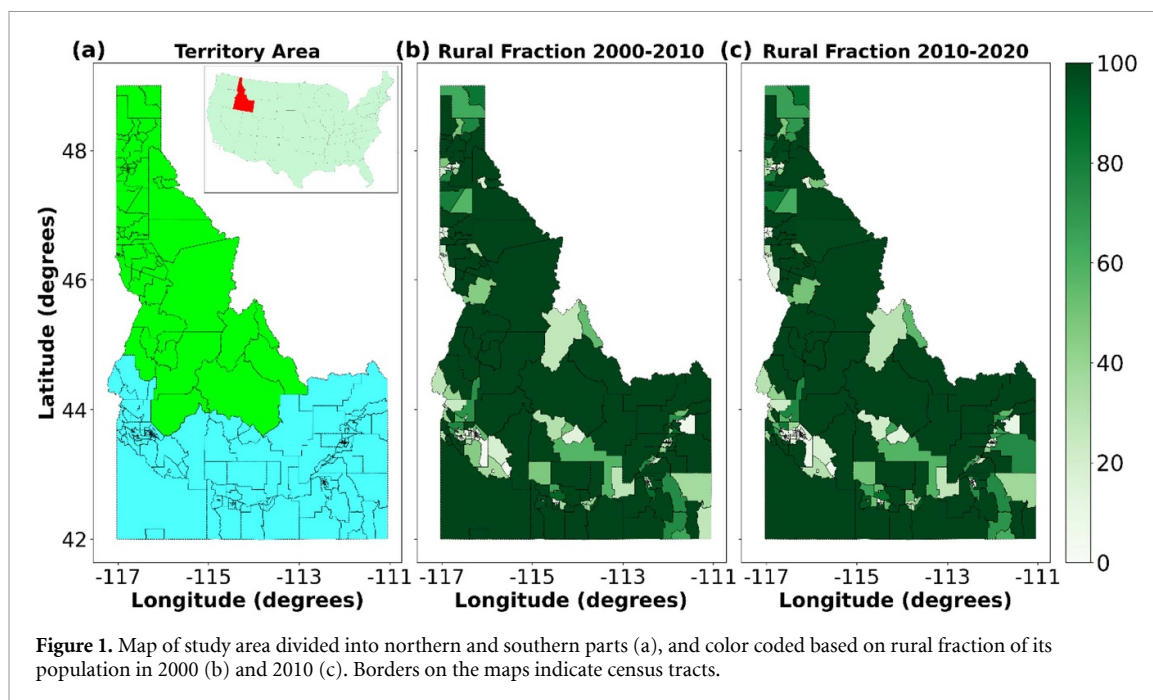


**Table 1.** Ecoclimatic and population characteristics of northern versus southern Idaho.

	Northern Idaho (NID)	Southern Idaho (SID)	References
Annual precipitation (2002–2020)	839 mm	409 mm	[28]
Summer daily average temperature (2002–2020)	16 °C	19 °C	[28]
Average elevation (range)	1599 m (216–3822)	1587 m (550–3711)	[29]
Forest cover in 2010	34%	6%	[30]
Total population in 2010	351 223	1217 698	[31–34]

the two regions. We conducted all our analyses at the census tract level and defined a census tract as ‘rural’, if more than 50% of its population are classified as rural in the decennial census data (2000, 2010, 2020).

## 2.2. Social and environmental variables

### 2.2.1. Air temperature

We used the GridMET dataset [28] which is a gridded meteorological dataset covering the contiguous US. It provides high-resolution (4 km) historical interpolated data from 1979–present, including variables such as temperature, precipitation, solar radiation, and humidity. This dataset is widely used for studying climate trends, modeling, and impact assessments [28]. We used daily air temperature from GridMET for the period of 2002–2020 to derive heatwaves (details later). We selected this period as a common timeline between different variables used in this study.

### 2.2.2. Land surface temperature (LST)

LST refers to the temperature of the Earth’s surface as measured from a satellite or ground-based instrument. LST helps determine heat impacts of local microclimates that may not be captured in mesoscale meteorological data such as GridMET [35, 36]. We used the MODIS satellite’s daily LST product (MOD11A1.061) with a spatial resolution of 1 km available from 2000–present [37]. We derived maximum June–August (summer) daily LST for each grid—i.e. single hottest LST during summer in each gridcell—and averaged them for each census tract annually during 2002–2020.

### 2.2.3. UHI

An UHI refers to the phenomenon where urban areas experience higher temperatures compared to their rural surroundings. This effect is primarily caused by built up areas such as buildings, roads, and infrastructure that absorb and retain heat, altering the local climate [38, 39]. We used the Global UHIs dataset of [38] with a spatial resolution of 300 m, available from 2003–2018. This dataset was developed

using the Surface UHI algorithm which, in simple terms, estimates the difference in LST between urban centers and surrounding rural areas [38, 39]. We adopted the annual average daytime UHI intensity (in °C) and averaged all grids in each census tract annually.

#### 2.2.4. Greenness

We derived Normalized Difference Vegetation Index—NDVI; a proxy for vegetation health—for each blockage-free 30 m pixel in Landsat satellite images (revisit time of 16 d) over Idaho during June–August (summer) from 2002–2020. We averaged NDVI for each pixel, and then averaged them over summer. Through extensive trial-and-error, we adopted a threshold of 0.3 for summer average NDVI (see figure S1 for more details), above which the urban green areas—irrigated in southern Idaho—can be separated from background vegetation. We then estimated the percentage of each census tract that was ‘green’ in each year.

#### 2.2.5. Ambient air quality, PM2.5

We used the daily, gridded surface PM2.5 data by Swanson *et al* [40] that is available at a 1 km resolution from 2003–2020. This data was developed for the western US through a geographically weighted regression algorithm using MODIS aerosol optical depth and meteorological data, and was also informed by inversion potential/strength [40]. We averaged PM2.5 estimates at the census tract level.

#### 2.2.6. Wildfire smoke

We used the daily estimates of wildfire smoke from Childs *et al* [41] who used a machine learning model informed by a combination of ground, satellite, and reanalysis data sources, including satellite-based aerosol optical depth, meteorological data, topography, atmospheric circulation trajectories, wildfire data, and ground observations of PM2.5 and smoke. This data is available daily at a 10 km resolution from 2006–2020 for contiguous US. We averaged smoke estimates at the census tract level.

#### 2.2.7. Social Vulnerability Index (SVI)

We used the nested hierarchical SVI from the US Centers for Disease Control and Prevention that amalgamates sixteen variables (e.g. income, employment, disability, seniority, minority) into four dimensions of ‘Socioeconomic Status’, ‘Household Composition and Disability’, ‘Minority Status and Language’, and ‘Housing Type and Transportation’. These four dimensions are then aggregated to the ‘Overall Vulnerability’ status. The overall vulnerability and its dimensions and subdimensions are normalized between 0 and 1 for Idaho, with 0 corresponding to least vulnerability and 1 associating with highest vulnerability across the state [42, 43]. We used available data from years 2000, 2010, 2014, 2016, 2018, 2020 for the periods 2002–2009, 2010–2013, 2014–2015, 2016–2017, 2018–2019, and 2020, respectively. We used census tract level overall SVI—finest resolution available—and assigned the SVI value to all residents of the census tract, acknowledging within tract heterogeneity. We also acknowledge that census tract boundaries can change between decennial census that can in turn impact the reported results.

#### 2.2.8. Rural–urban fraction

We used Decennial Demographic and Housing Characteristics (P2) data from 2000 (for years 2000–2009), 2010 (for years 2010–2019) and 2020 (for year 2020) to estimate the fraction of rural population in each census tract.

#### 2.2.9. Population

We used the annual gridded population data from WorldPop [33] that disaggregates census-reported population to 92 m grids using a machine learning model, informed by a variety of covariates including roads, land cover, built structures, cities or urban areas, night-time lights, infrastructure, environmental data, protected areas, and water bodies [44]. Using this gridded dataset is specifically helpful for collocating populations with climate-related extremes to accurately estimate exposure to hazards.

### 2.3. Methods

#### 2.3.1. Heatwave exposure

We defined heatwave events as a prolonged period of hot weather with maximum daily temperatures exceeding 90 °F (32.22 °C) for at least three consecutive days. This definition is aligned with moderate impacts of heatwaves on human health and infrastructure [45]. We also used a spatiotemporally localized approach to define heatwaves, using the 95th percentile of the long-term daily temperature time series of each day and each grid as the threshold. A 3 d consecutive exceedance is a requirement in the localized heatwave definition as well. We developed daily binary heatwave maps, which we then overlaid on

population maps to estimate daily heatwave exposures. We down-sampled the 4 km binary heatwave grids to the 92 m population grids, and estimated the number of people exposed to heatwaves in each 92 m grid-cell. We subsequently aggregated (through a summation) daily heatwave exposures at the census tract and annual scales, returning the annual number of person-days exposure to heatwave. Heatwave exposure trends can be driven by trends in the number of heatwave days and trends in population.

### 2.3.2. Spatial aggregation

We aggregated all environmental and social variables to the census tract level. In doing so, all grid-cells with center points within the shapefile of the census tract were aggregated—i.e. summed in the case of heatwave exposure and averaged for all other variables. Census tracts can change from one decennial census to another, and we adopted the shapefiles associated with each census tract for the year of analysis. We recognize that not only the source data are associated with uncertainty, but also the overlaying of various raster and shapefile data can introduce additional uncertainties.

### 2.3.3. Trend analysis

We used the linear least squares regression to calculate trends in social and environmental variables.

Given our interest in trends of heat and smoke indicators with human health and livelihood relevance, we adopt population-weighted trends, where indicated in the Results section. Population-weighted trends provide a reliable indicator for human impact studies because they incorporate where people live and are exposed to health-implicating environmental factors. By weighting trends based on population distribution, these analyses reflect the true potential risk faced by communities [46, 47]. Additionally, population-weighted trends can help prioritize interventions and adaptation strategies in areas where they are most needed to protect vulnerable populations from the impacts of extremes [48–50].

We applied the population-weighting scheme to each variable at the census tract level, before trend analyses:

$$\text{Population-weighted aggregation} = \frac{\sum_{i=1}^N \zeta_i \times \eta_i}{\sum_{i=1}^N \eta_i} \quad (1)$$

where  $\zeta$  is the variable of interest (e.g. LST-Max) for census tract  $i$ ,  $\eta$  denotes population of census tract  $i$ , and  $N$  is the total number of census tracts. This aggregation was conducted for each variable of interest in each year. We also added area-weighted results for completeness.

Finally, we used t-test to assess the null hypothesis that two independent samples have identical average. Here too, we used a two-sided  $p$ -value to determine statistical significance.

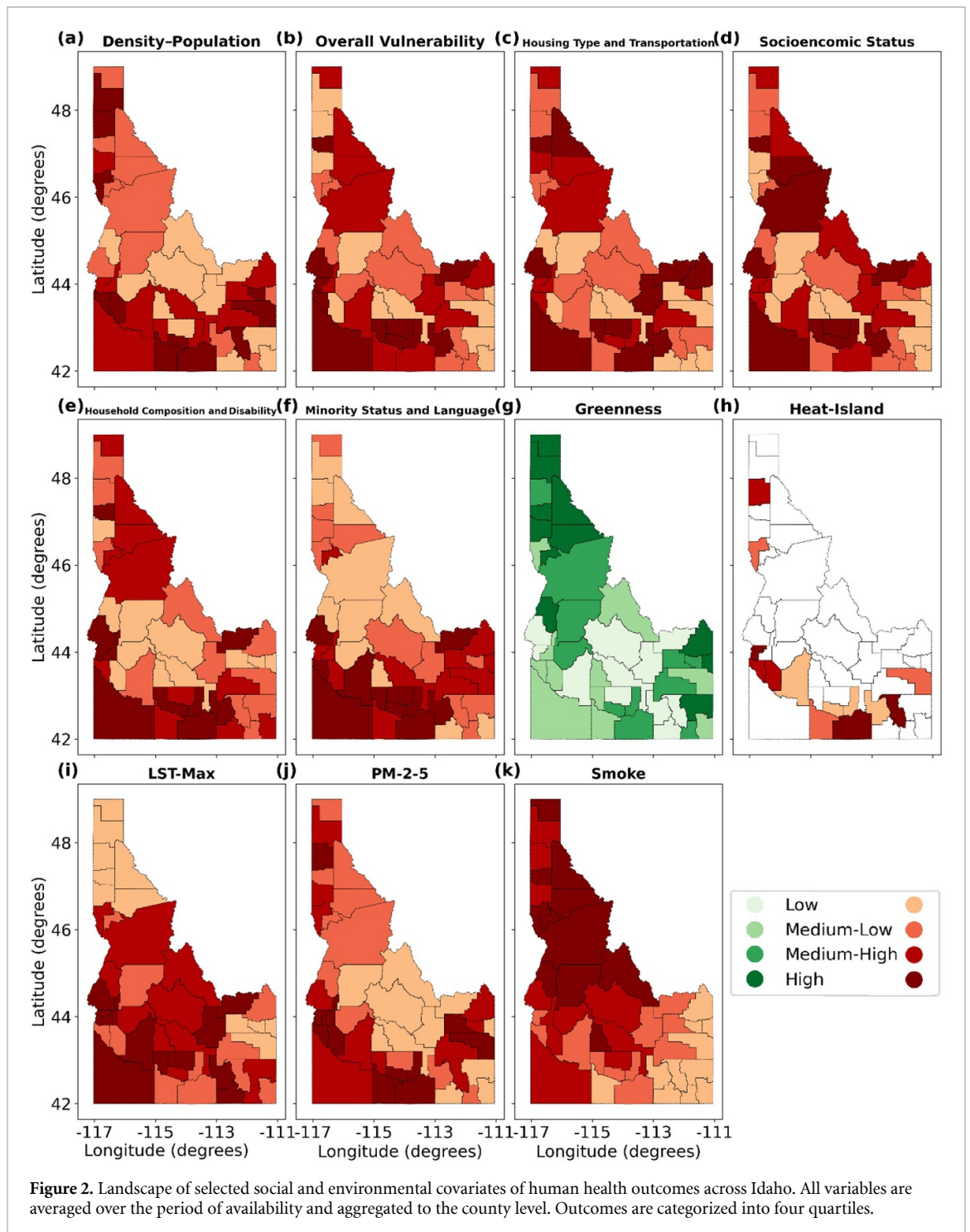
## 3. Results and discussion

### 3.1. Patterns of heat and wildfire smoke indicators

We first examine the landscape of social and environmental variables at the county-level for the period of 2002–2020. Since census tract perimeters can change from one decade to another, we averaged all variables at the county level for the period of study, and then classified them into four categories of low, medium-low, medium-high, and high using quartiles of each variable (figure 2). An absolute majority of high-vulnerability counties occurred in southern Idaho (SID) (figure 2(b)), where LST-Max (figure 2(i)), heat island (figure 2(h)), PM2.5 (figure 2(j)) and population density (figure 2(a)) were also highest. Heat-related variables in particular, and to some extent other variables, are modulated by latitudinal- and elevational-driven climatic and biological factors. Notably, wildfire smoke concentration was highest in northern Idaho (NID) (figure 2(k)), coincident with high socioeconomic vulnerability (figure 2(d)). Local economies in NID are greatly dependent on natural resources, including tourism, and are impacted by extended periods of wildfire smoke blanketing the region.

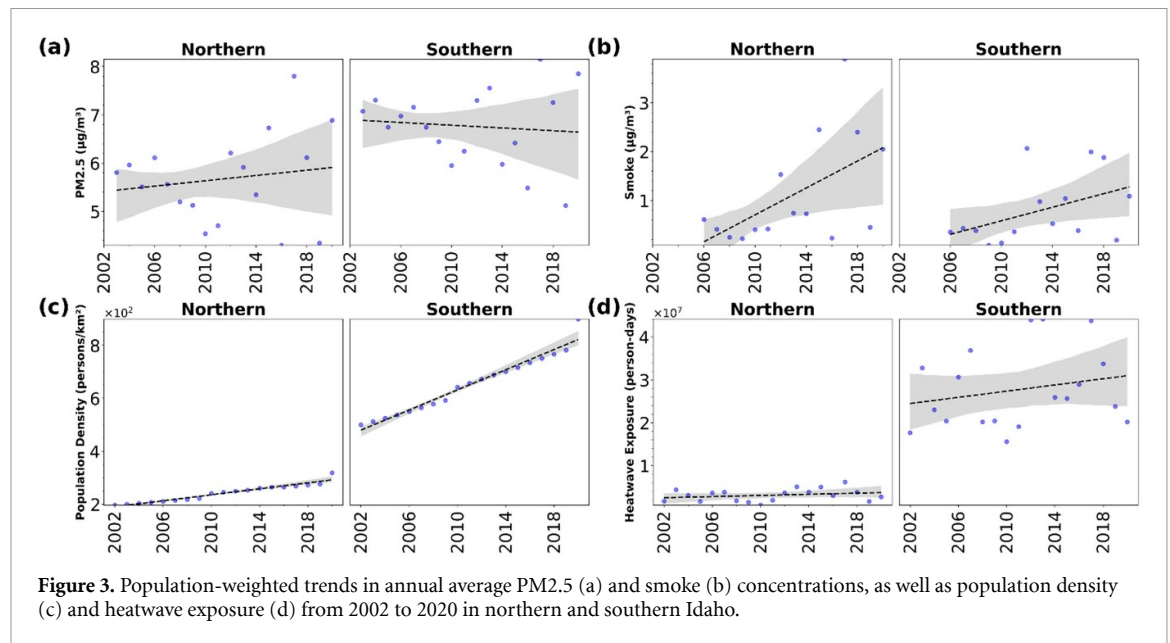
### 3.2. Trends of heat and wildfire smoke indicators

Population-weighted wildfire smoke, and heatwave exposure, showed positive trends across Idaho. Both the long-term average and the trend in annual average smoke concentration in NID were higher than those in SID (figures 3(a) and (b)). In NID, the population-weighted annual average smoke concentrations from 2006 to 2020 was  $1.12 \frac{\mu\text{g}}{\text{m}^3}$ , as compared to  $0.79 \frac{\mu\text{g}}{\text{m}^3}$  in SID, although the difference did not reach statistical significance (two-sided t-test  $p$ : 0.34). To put these numbers in perspective, the US Environmental Protection Agency's standard for annual average PM2.5 is  $9 \frac{\mu\text{g}}{\text{m}^3}$ ; and this is from all sources, not only smoke [51]. The



trend in annual average smoke concentration was statistically significant ( $0.14 \frac{\mu\text{g}}{\text{m}^3} \text{yr}^{-1}$ ; two-sided  $p$ : 0.03) in NID, but not in SID ( $0.07 \frac{\mu\text{g}}{\text{m}^3} \text{yr}^{-1}$ ; two-sided  $p$ : 0.09). Statistical significance is shadowed by the short length of the observations and large interannual variability. We note that lack of statistical significance does not indicate lack of impact [52], and that trend analysis over longer intervals (e.g. 3 year moving average) will render statistical significance. Here, we are specifically interested in the interannual variability of wildfire smoke; while this variability shadows the statistical significance, years of high smoke exposure are becoming more frequent in Idaho due to increasing wildfire activity and years of low smoke exposure are becoming increasingly rare [53, 54].

Patterns were contrasting for ambient air quality compared to smoke, with population-weighted annual average PM<sub>2.5</sub> being higher in SID (6.76 versus  $5.67 \frac{\mu\text{g}}{\text{m}^3}$ , two-sided  $p$ : 0.00). Trends of population-weighted PM<sub>2.5</sub> were also contrasting compared to those of smoke, with annual ambient air quality improving in SID while deteriorating in NID (neither one was statistically significant). We acknowledge that the data sources



for total PM<sub>2.5</sub> and smoke PM<sub>2.5</sub> are different, and caution should be adopted when comparing ambient air quality patterns and trends with those of smoke. Improving trends of air quality in the south, where population density is much higher (table 1), are likely driven by regulatory efforts focused on reducing anthropogenic sources. Heatwave exposure also increased in SID (361 000 person-days yr<sup>-1</sup>) and NID (66 000 person-days yr<sup>-1</sup>), although neither one reached statistical significance due to short data length, large interannual variability, moderate definition of heatwaves (max daily temperature above 90 °F), and using interpolated data that are known to dampen extremes observed in station data [55, 56].

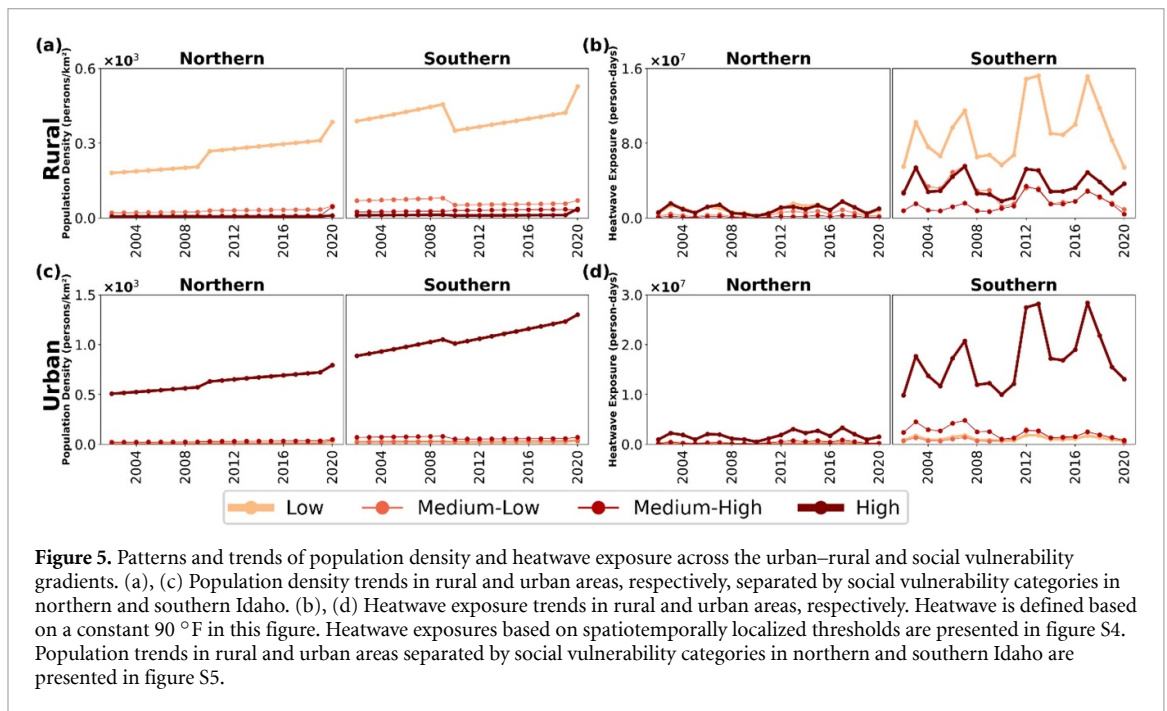
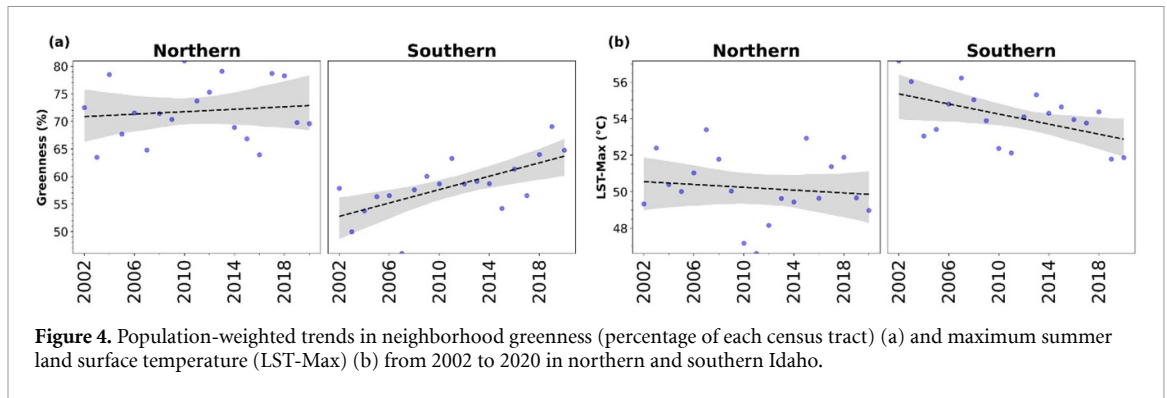
Figure S2 shows area-weighted trends of PM<sub>2.5</sub> and wildfire smoke in Idaho, with generally similar patterns and some nuanced differences to those of population-weighted trends in figure 3. Population-weighted PM<sub>2.5</sub> in NID shows a marginally increasing trend (figure 3(a)), while area-weighted PM<sub>2.5</sub> shows a marginally declining trend (figure S2(a)) [57].

While GridMET-based heatwave exposure showed a positive trend in par with global and regional warming trends, population-weighted LST-Max showed a negative trend in SID ( $-0.14$  °C yr<sup>-1</sup>; two-sided  $p = 0.02$ ) and a rather stable trend with a marginal decline in NID ( $-0.04$  °C yr<sup>-1</sup>; two-sided  $p = 0.63$ ) (figure 4). This was coincident with increasing neighborhood greenness in SID (0.61% per year; two-sided  $p = 0.00$ ) and stable greenness in NID (marginal increase of 0.11% per year; two-sided  $p = 0.64$ ) (figure 4). We note that the 4 km resolution of GridMET does not capture some of the microclimatic effects that are captured at the finer resolution of LST-Max. SID, specifically, has been undergoing a major land cover change, and new developments with irrigated green spaces have been increasingly replacing barren lands. Long-term average LST-Max was higher and greenness was lower in SID compared to NID, due to ecoclimatic, latitudinal and elevational gradients. Area-weighted LST-Max and greenness are shown in figure S3.

### 3.3. Trends of heat and wildfire smoke indicators across social vulnerability and rural–urban gradients

Trends and patterns of exposure to heat and wildfire smoke showed distinct differences between rural and urban centers and across social vulnerability gradients (figures 5–7). Conspicuously, the population density for the low vulnerability class in rural areas was associated with a higher long-term average and a higher positive trend both for SID and NID (figure 5(a)). Note that population density in rural areas is lower than urban areas, and here we do not cross-compare population densities between rural and urban areas. Our referral to high population density in rural areas is only in a relative sense. In urban areas, the high vulnerability class lived in higher density communities and observed a larger rate of population density increase (figure 5(c)). Heatwave exposures—defined based on the constant 90 °F threshold—followed a similar pattern to population density in SID, but not NID, driven by ecoclimatic conditions. In hotter SID region, low vulnerability populations in rural and high vulnerability populations in urban areas were associated with higher cumulative exposures (9.2 million versus 19.9 million person-days) and a larger rate





of increase (155 800 versus 463 500 person-days  $\text{yr}^{-1}$ ; neither was statistically significant at the 5% level although effect size is notable—lack of significance is attributed to interannual variability) from 2002 to 2020 (figures 5(b) and (d)). In the colder and wetter NID region, where a majority of population lives in valleys in proximity of water bodies, heatwave exposure patterns and trends were not as distinct between different vulnerability classes (figures 5(b) and (d)).

Population-weighted annual average PM<sub>2.5</sub> concentration had a similar pattern to those of population density both in SID and NID, with the low vulnerability group in NID and high vulnerability group in SID being exposed to poorer ambient air quality (figures 6(a) and (c)). There is not a marked difference between the trends of population-weighted PM<sub>2.5</sub> across vulnerability groups from 2002 to 2020.

Population-weighted annual average wildfire smoke concentration, however, was similar between different vulnerability groups both in terms of long-term average and trends (figures 6(b) and (d)). Area-weighted PM<sub>2.5</sub> and smoke results are shown in figure S6.

Neighborhood greenness—i.e. fraction of land area in each census tract with mean summer NDVI  $\geq 0.3$ —generally showed a positive trend in SID for all social vulnerability groups and for both rural and urban areas (figures 7(a) and (c)). This increasing greenness in SID was coincident with declining LST-Max across all vulnerability groups and for both rural and urban areas (figures 7(b) and (d)). In NID, however, greenness and LST-Max trends were not associated with conspicuous trends (figure 7), in part due to the background ecoclimatic conditions (table 1). Contrary to expectations, long-term average LST-Max in high vulnerability urban areas of SID (figure 7(d)) was lower than that of low vulnerability areas, although

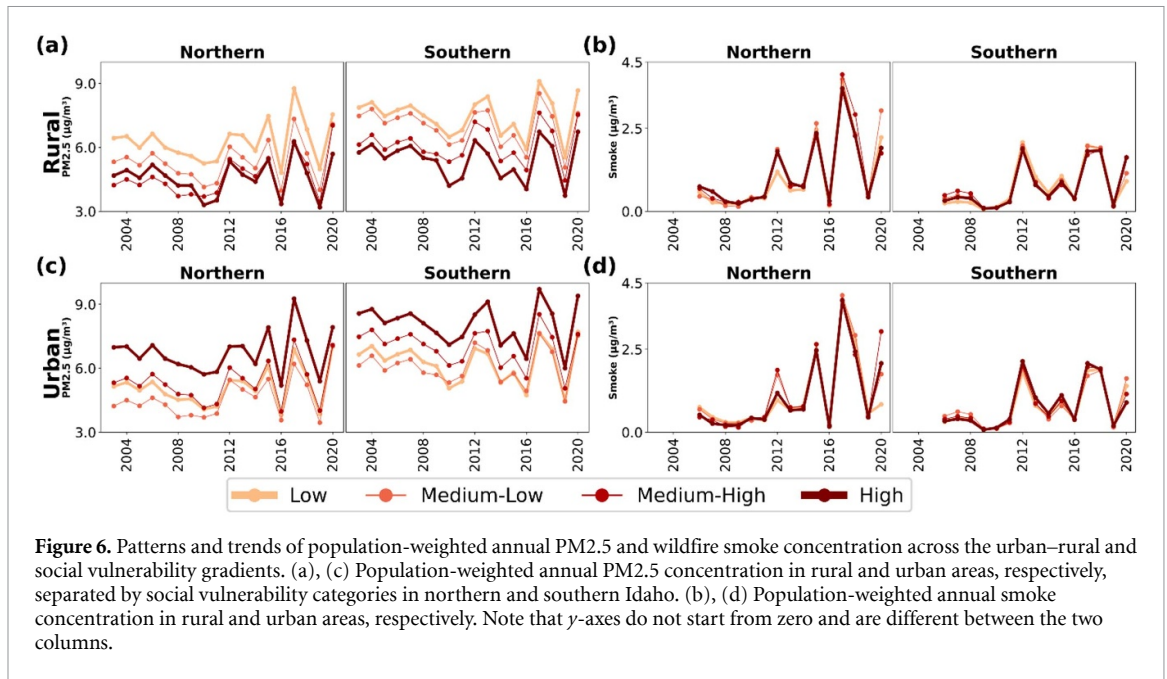


**Figure 6.** Patterns and trends of population-weighted annual PM<sub>2.5</sub> and wildfire smoke concentration across the urban-rural and social vulnerability gradients. (a), (c) Population-weighted annual PM<sub>2.5</sub> concentration in rural and urban areas, respectively, separated by social vulnerability categories in northern and southern Idaho. (b), (d) Population-weighted annual smoke concentration in rural and urban areas, respectively. Note that y-axes do not start from zero and are different between the two columns.

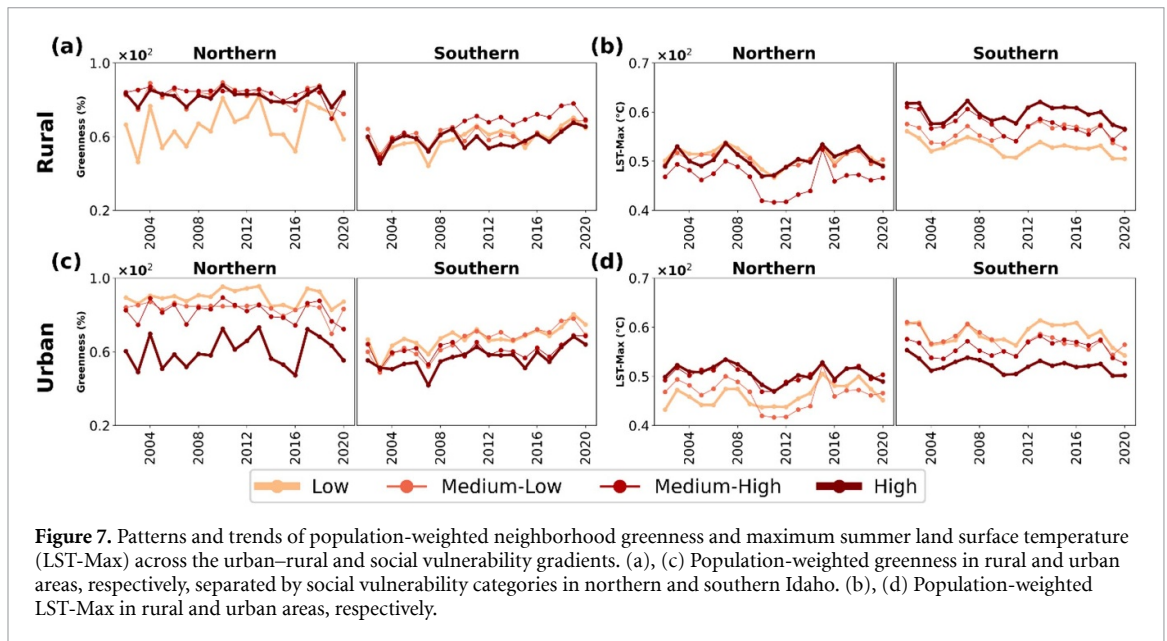
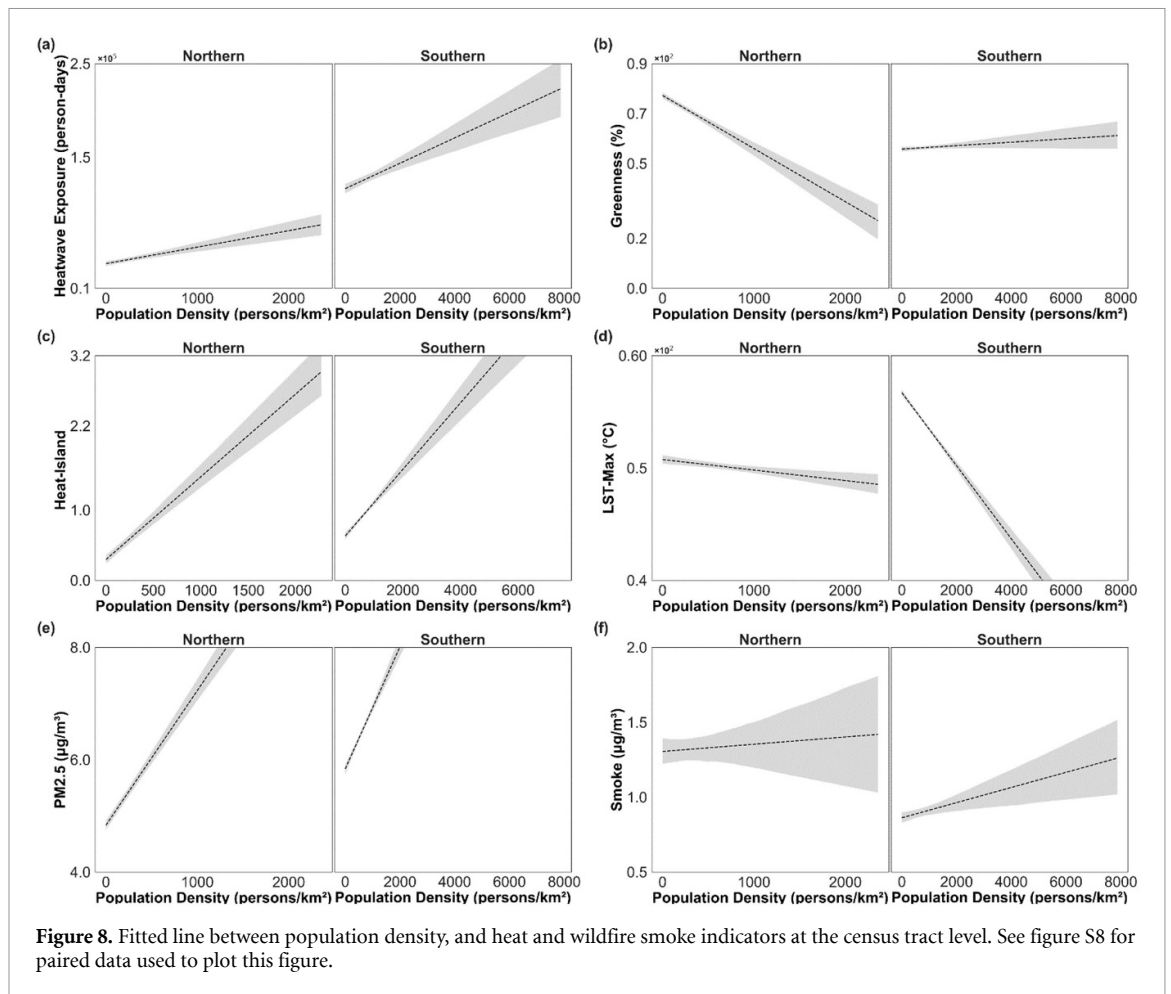


**Figure 7.** Patterns and trends of population-weighted neighborhood greenness and maximum summer land surface temperature (LST-Max) across the urban-rural and social vulnerability gradients. (a), (c) Population-weighted greenness in rural and urban areas, respectively, separated by social vulnerability categories in northern and southern Idaho. (b), (d) Population-weighted LST-Max in rural and urban areas, respectively.

the long-term average greenness was also lower. This is because a majority of high vulnerability urban census tracts occur in the western SID, which is associated with lower elevations and hotter-drier hydroclimate conditions. Area-weighted greenness and LST-Max results are shown in figure S7. Area-weighted greenness was lower than population-weighted greenness (figure 7), and area-weighted LST-Max was higher than population-weighted LST-Max.

### 3.4. Social and environmental covariates of heat and wildfire smoke

Here we explore linear relationships between census tract-level population density and various indicators of heat and smoke. Increase in population density was associated with an increase in heatwave exposure (SID:  $r = 0.09$ ,  $p = 0.00$ ; NID:  $r = 0.18$ ,  $p = 0.00$ ), UHI intensity (SID:  $r = 0.43$ ,  $p = 0.00$ ; NID:  $r = 0.40$ ,  $p = 0.00$ ), smoke (SID:  $r = 0.05$ ,  $p = 0.00$ ; NID:  $r = 0.02$ ,  $p = 0.59$ ), and PM<sub>2.5</sub> (SID:  $r = 0.50$ ,  $p = 0.00$ ; NID:  $r = 0.59$ ,  $p = 0.00$ ). Lower correlation values despite statistical significance (e.g. population density and heatwave exposure) indicates that the effect size might be limited, although the impact might be large. Specifically, a 1000 persons km<sup>-2</sup> increase in population density was associated with an increase in the intensity of UHI by 0.47 °C in SID and 1.18 °C in NID. Furthermore, as population density increased, neighborhood greenness in NID—which is to a large extent natural—declined, whereas anthropogenic

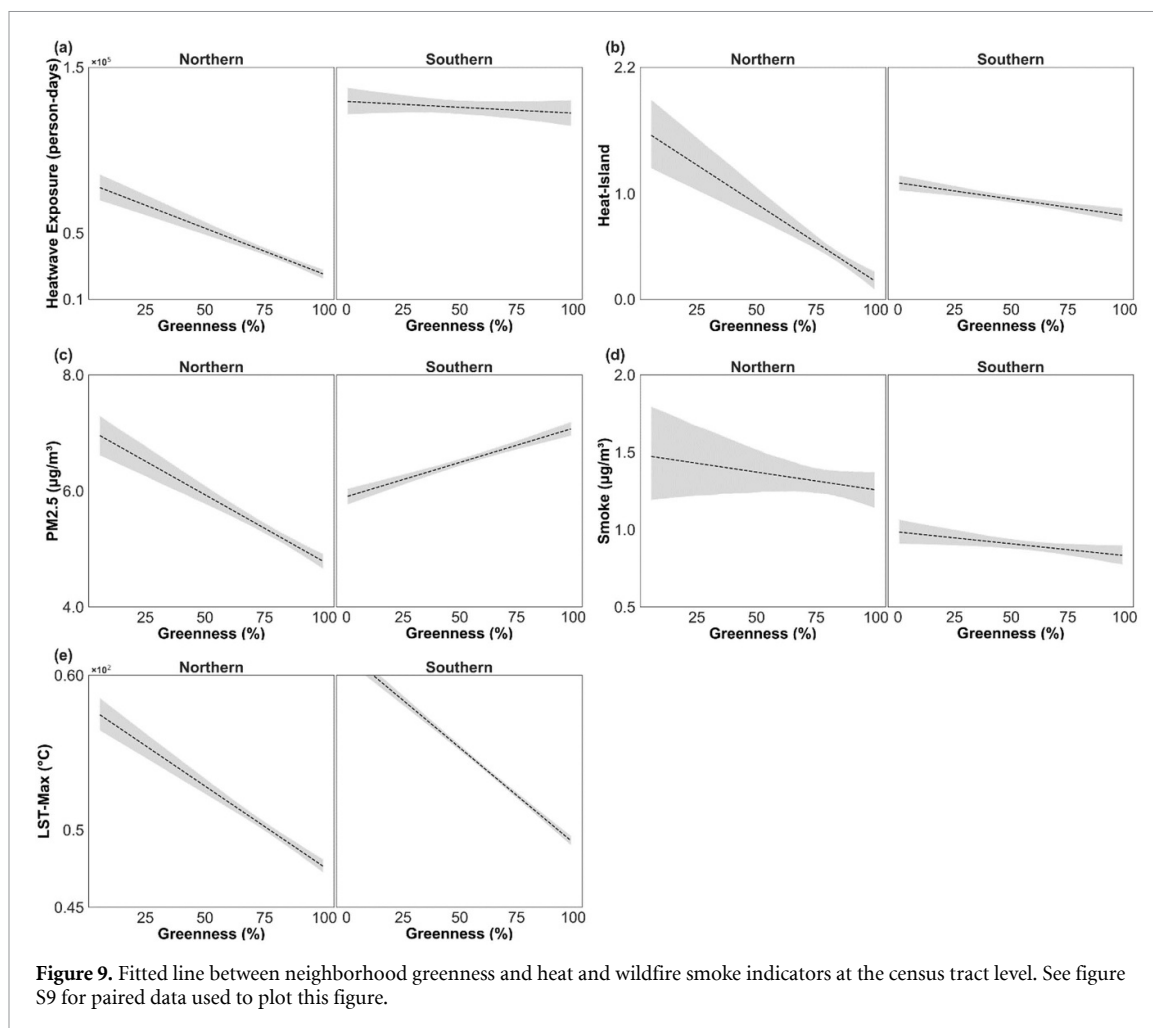


greenness in SID—irrigation-sourced—increased (figure 8(b)). Moreover, population density and LST-Max were negatively correlated in SID (figure 8(d);  $r = -0.45$ ,  $p = 0.00$ ), coincident with increasing greenness with population density (figure 8(b)).

Finally, increasing neighborhood greenness was associated with a decline in heatwave exposure (SID:  $r = -0.01$ ,  $p = 0.40$ ; NID:  $r = -0.28$ ,  $p = 0.00$ ), heat island intensity (SID:  $r = -0.08$ ,  $p = 0.00$ ; NID:  $r = -0.26$ ,  $p = 0.00$ ), LST-Max (SID:  $r = -0.49$ ,  $p = 0.00$ ; NID:  $r = -0.38$ ,  $p = 0.00$ ), and smoke (SID:  $r = -0.05$ ,  $p = 0.01$ ; NID:  $r = -0.04$ ,  $p = 0.22$ ) (figure 9). Specifically, a 10% increase in neighborhood greenness in SID and NID was coincident with a decline of  $0.03^\circ\text{C}$  and  $0.15^\circ\text{C}$  in the UHI intensity, respectively. The relationship between greenness and PM2.5, however, was not monotonic across SID and NID. Over NID, increasing greenness indicated lower population density and lower anthropogenic sources of air pollution, whereas this relationship was reversed in SID where population density increases with greenness (figure 9).

#### 4. Conclusion

Evidence of climate extreme impacts on human communities is widespread and mounting [58], with a larger burden on the most vulnerable populations [59]. Here, we focused on heat and wildfire smoke indicators in Idaho and how they differentially impacted people across the urban–rural and social vulnerability gradients in the last two decades. Our results showed that low vulnerability rural populations had a higher long-term average and trend of exposure to heatwaves in southern Idaho, while the average and trend of exposure to heatwaves were greater for high vulnerability urban populations in the region. The contrast between rural and urban populations may be masked in other reported studies, given rural populations only account for one-fifth of the US population and rurality is often not explicitly included in analyses [9]. While biophysical characteristics of urban areas can amplify various climatic hazards, for example through heat island impacts, separating rural from urban impacts is of great importance, given rural communities face unique challenges in adapting to, responding to and recovering from disasters [60], mainly due to limited resources, including access to healthcare, emergency services, and civil infrastructure [61, 62]. The sparse population in rural



areas can lead to longer response times and difficulties in accessing aid during emergencies [63]. Moreover, the economic dependence on agriculture and natural resources makes rural communities especially vulnerable to the impacts of climate-related disasters, such as extreme weather events or wildfires, which can devastate livelihoods and exacerbate existing socioeconomic disparities [64].

Annual average PM<sub>2.5</sub> concentration and population density were greatest for high vulnerability populations across urban centers in Idaho. In rural areas, however, PM<sub>2.5</sub> and population density were highest for low vulnerability populations. Wildfire smoke was uniform across all vulnerability classes over Idaho. We note that although regional smoke concentrations are similar for different strata of population, housing may be less well-sealed and lack air conditioning or air filtration systems in low income communities, and hence residents may be more likely to experience higher levels of indoor smoke exposure during wildfires [65]. High income communities with better housing infrastructure may still face smoke infiltration, but residents often have more resources to implement protective measures such as air purifiers or HVAC systems, reducing indoor air pollution levels [66]. Population-weighted air quality generally improved in southern Idaho from 2003 to 2020, in par with national trends, mainly due to regulatory efforts [67]; but this trend did not hold in northern Idaho. Wildfire smoke concentrations increased across Idaho, and was associated with pronounced trends in northern Idaho over the past two decades. Wildfire emissions have reversed some of the progress in improving air quality across the US [41].

While mesoscale heat indicators in Idaho showed an increasing trend, consistent with regional warming trends, population-weighted maximum summer LST was associated with a decline in the past two decades coincident with increasing neighborhood greening due to converting barren and agricultural lands to subdivisions with irrigated lawn, trees, and other green aesthetic features. Neighborhood greening, such as planting trees and creating green spaces, is a valuable mitigative action for climate change and heat [68]. Trees and vegetation provide shade, reduce surface temperatures, and help cool the air through evapotranspiration, mitigating the UHI effect. Green infrastructure can also improve air quality, enhance biodiversity, and promote community well-being, making neighborhoods more resilient to extreme heat events and climate impacts [69, 70]. Additionally, exposure to green spaces has been linked to reduced

heat-related illnesses, cardiovascular problems, and respiratory issues [71, 72], highlighting the importance of urban greening initiatives for promoting public health resilience [73]. Implementing neighborhood greening initiatives can contribute to overall climate adaptation strategies, fostering more sustainable and livable urban environments. This effective mitigation strategy, however, is water intensive and should be carefully considered in drought-stricken areas in the western US.

### Data availability statement

All data that support the findings of this study are included within the article (and any supplementary information files).

### Acknowledgment

This study was supported by the Boise State University Healthy Idaho Grand Initiative. M S and J T A also received support from the US Joint Fire Science Program (U.S. Department of the Interior/Bureau of Land Management) Grant L21AC10247.

### Conflict of interest

The authors declare no conflicts of interest relevant to this study.

### Open research

All source data used in this study are publicly and freely available:

GridMET: `ee.ImageCollection('IDAHO_EPSCOR/GRIDMET')`.

MODIS LST: `ee.ImageCollection('MODIS/061/MYD11A1')`.

Landsat: `ee.ImageCollection('LANDSAT/LC08/C01/T1_8DAY_NDVI')`.

PM2.5: [https://springernature.figshare.com/collections/Daily\\_1-kilometer\\_PM2\\_5\\_maps\\_accounting\\_for\\_inversion\\_potentials\\_for\\_the\\_western\\_United\\_States\\_2003-2020/5562330/1](https://springernature.figshare.com/collections/Daily_1-kilometer_PM2_5_maps_accounting_for_inversion_potentials_for_the_western_United_States_2003-2020/5562330/1).

Wildfire smoke: [www.stanforddecholab.com/wildfire\\_smoke](http://www.stanforddecholab.com/wildfire_smoke).

Population: [www.worldpop.org/](http://www.worldpop.org/).

Urban heat island: `ee.ImageCollection('YALE/YCEO/UHI/Summer_UHI_yearly_pixel/v4')`.

Social Vulnerability Index: [www.atsdr.cdc.gov/placeandhealth/svi/index.html](http://www.atsdr.cdc.gov/placeandhealth/svi/index.html).

### Author credits

Conceptualization: S T S, J P, J T A, E S, A R, H F, S W, E H, B C, M S.

Data curation: S T S.

Formal analysis: S T S.

Funding acquisition: M S, J P, H F, E S.

Investigation: S T S, M S, J T A.

Methodology: S T S, M S.

Project administration: M S.

Resources: J P, M S.

Software: S T S.

Supervision: M S.

Validation: S T S, M S.

Visualization: S T S.

Writing—original draft: S T S, J P, J T A, E S, A R, H F, S W, E H, B C, M S.

Writing—review & editing: N A.

### ORCID iDs

Seyd Teymoor Seydi  <https://orcid.org/0000-0002-3678-4877>

John T Abatzoglou  <https://orcid.org/0000-0001-7599-9750>

Mojtaba Sadegh  <https://orcid.org/0000-0003-1775-5445>

## References

- [1] Ebi K L, Ogden N H, Semenza J C and Woodward A 2017 Detecting and attributing health burdens to climate change *Environ. Health Perspect.* **125** 085004
- [2] Dilling L, Pizzi E, Berggren J, Ravikumar A and Andersson K 2017 Drivers of adaptation: responses to weather- and climate-related hazards in 60 local governments in the Intermountain Western U.S *Environ. Plan. A* **49** 2628–48
- [3] Dilling L, Daly M E, Travis W R, Wilhelmi O V and Klein R A 2015 The dynamics of vulnerability: why adapting to climate variability will not always prepare us for climate change *WIREs Clim. Change* **6** 413–25
- [4] Vogel E, Donat M G, Alexander L V, Meinshausen M, Ray D K, Karoly D, Meinshausen N and Frieler K 2019 The effects of climate extremes on global agricultural yields *Environ. Res. Lett.* **14** 054010
- [5] Yoo E-H, Roberts J E, Eum Y, Li X, Chu L, Wang P and Chen K 2022 Short-term exposure to air pollution and mental disorders: a case-crossover study in New York City *Environ. Res.: Health* **1** 015001
- [6] Vrac M and Naveau P 2007 Stochastic downscaling of precipitation: from dry events to heavy rainfalls *Water Resour. Res.* **43** 2006WR005308
- [7] Gasparrini A, Guo Y, Hashizume M, Lavigne E, Zanobetti A, Schwartz J, Tobias A, Tong S, Rocklöv J and Forsberg B 2015 Mortality risk attributable to high and low ambient temperature: a multicountry observational study *Lancet* **386** 369–75
- [8] Hasan F, Marsia S, Patel K, Agrawal P and Razzak J A 2021 Effective community-based interventions for the prevention and management of heat-related illnesses: a scoping review *Int. J. Environ. Res. Public Health* **18** 8362
- [9] Modaresi Rad A et al 2023 Social vulnerability of the people exposed to wildfires in U.S. West Coast states *Sci. Adv.* **9** eadh4615
- [10] D'Evelyn S M et al 2022 Wildfire, smoke exposure, human health, and environmental justice need to be integrated into forest restoration and management *Curr. Environ. Health Rep.* **9** 366–85
- [11] Falchetta G, De Cian E, Sue Wing I and Carr D 2024 Global projections of heat exposure of older adults *Nat. Commun.* **15** 3678
- [12] Alizadeh M R, Abatzoglou J T, Adamowski J F, Prestemon J P, Chittoori B, Akbari Asanjan A and Sadegh M 2022 Increasing heat-stress inequality in a warming climate *Earth's Future* **10** e2021EF002488
- [13] Hopfer S, Jiao A, Li M, Vargas A L and Wu J 2024 Repeat wildfire and smoke experiences shared by four communities in Southern California: local impacts and community needs *Environ. Res.: Health* **2** 035013
- [14] Cutter S L and Finch C 2008 Temporal and spatial changes in social vulnerability to natural hazards *Proc. Natl Acad. Sci. USA* **105** 2301–6
- [15] Martinich J, Neumann J, Ludwig L and Jantarasami L 2013 Risks of sea level rise to disadvantaged communities in the United States *Mitig. Adapt. Strateg. Glob. Change* **18** 169–85
- [16] O'Neill M S and Ebi K L 2009 Temperature extremes and health: impacts of climate variability and change in the United States *J. Occup. Environ. Med.* **51** 13–25
- [17] Modaresi Rad A, Abatzoglou J T, Kreitler J, Alizadeh M R, AghaKouchak A, Hudyma N, Nauslar N J and Sadegh M 2023 Human and infrastructure exposure to large wildfires in the United States *Nat. Sustain.* **6** 1343–51
- [18] Smith K R, Woodward A, Campbell-Lendrum D, Chadee D D, Honda Y, Liu Q, Olwoch J M, Revich B, Sauerborn R and Aranda C 2014 Climate change 2014: impacts, adaptation, and vulnerability. Part A: global and sectoral aspects. *Contribution of Working Group II to the fifth assessment report of the Intergovernmental Panel on Climate Change*
- [19] Reid C E, Considine E M, Watson G L, Telesca D, Pfister G G and Jerrett M 2023 Effect modification of the association between fine particulate air pollution during a wildfire event and respiratory health by area-level measures of socio-economic status, race/ethnicity, and smoking prevalence *Environ. Res.: Health* **1** 025005
- [20] Lambrou N, Kolden C, Loukaitou-Sideris A, Anjum E and Acey C 2023 Social drivers of vulnerability to wildfire disasters: a review of the literature *Landscape Urban Plan.* **237** 104797
- [21] Flanagan B E, Gregory E W, Hallisey E J, Heitgerd J L and Lewis B 2011 A social vulnerability index for disaster management *J. Homeland Secur. Emerg. Manage.* **8** 0000102202154773551792
- [22] Wang S, Zhang M, Huang X, Hu T, Sun Q C, Corcoran J and Liu Y 2022 Urban–rural disparity of social vulnerability to natural hazards in Australia *Sci. Rep.* **12** 13665
- [23] USGCRP 2023 *Fifth National Climate Assessment* (U.S. Global Change Research Program)
- [24] Engle N L, De Bremond A, Malone E L and Moss R H 2014 Towards a resilience indicator framework for making climate-change adaptation decisions *Mitig. Adapt. Strateg. Glob. Change* **19** 1295–312
- [25] Abatzoglou J T, Marshall A M and Harley G L 2021 Observed and projected changes in Idaho's climate *Idaho Climate-Economy Impacts Assessment* (available at: [www.uidaho.edu/-/media/UIDaho-Responsive/Files/president/direct-reports/mcclure-center/iceia/iceia-climate-report-2021.pdf](http://www.uidaho.edu/-/media/UIDaho-Responsive/Files/president/direct-reports/mcclure-center/iceia/iceia-climate-report-2021.pdf))
- [26] McClure C D and Jaffe D A 2018 US particulate matter air quality improves except in wildfire-prone areas *Proc. Natl Acad. Sci. USA* **115** 7901–6
- [27] Dieter C A 2018 *Water Availability and Use Science Program: Estimated Use of Water in the United States in 2015* (Geological Survey)
- [28] Abatzoglou J T 2013 Development of gridded surface meteorological data for ecological applications and modelling *Int. J. Climatol.* **33** 121–31
- [29] 2014 Copernicus DEM GLO-30: Global 30m digital elevation model *Google for Developers* (available at: [https://developers.google.com/earth-engine/datasets/catalog/COPERNICUS\\_DEM\\_GLO30](https://developers.google.com/earth-engine/datasets/catalog/COPERNICUS_DEM_GLO30))
- [30] Sexton J O et al 2013 Global, 30-m resolution continuous fields of tree cover: Landsat-based rescaling of MODIS vegetation continuous fields with lidar-based estimates of error *Int. J. Digit. Earth* **6** 427–48
- [31] Gaughan A E, Stevens F R, Linard C, Jia P and Tatem A J 2013 High resolution population distribution maps for Southeast Asia in 2010 and 2015 *PLoS One* **8** e55882
- [32] Linard C, Gilbert M, Snow R W, Noor A M and Tatem A J 2012 Population distribution, settlement patterns and accessibility across Africa in 2010 *PLoS One* **7** e31743
- [33] 2018 Anon Open Spatial Demographic Data and Research *WorldPop* (available at: [www.worldpop.org/](http://www.worldpop.org/))
- [34] Sorichetta A, Hornby G M, Stevens F R, Gaughan A E, Linard C and Tatem A J 2015 High-resolution gridded population datasets for Latin America and the Caribbean in 2010, 2015, and 2020 *Sci. Data* **2** 1–12
- [35] Nguyen B M, Tian G, Vo M-T, Michel A, Corpetti T and Granero-Belinchon C 2022 Convolutional neural network modelling for MODIS land surface temperature super-resolution 2022 *30th European Signal Processing Conf. (EUSIPCO)* (IEEE) pp 1806–10
- [36] Seydi S T, Abatzoglou J T, AghaKouchak A, Pourmohamad Y, Mishra A and Sadegh M 2024 Predictive understanding of links between vegetation and soil burn severities using physics-informed machine learning *Earth's Future* **12** e2024EF004873

- [37] Zhengming W, Simon H and Glynn H 2015 MOD11A1 MODIS/terra land surface temperature/emissivity daily L3 global 1 km SIN grid V006 NASA EOSDIS Land Processes DAAC (<https://doi.org/10.5067/modis/mod11c1.006>)
- [38] Chakraborty T and Lee X 2023 Documentation for the Yale Center for Earth Observation (YCEO) surface urban heat islands Version 4 2003–18 (available at: <https://sedac.ciesin.columbia.edu/downloads/docs/sdei/sdei-yceo-sfc-uhi-v4-documentation.pdf>)
- [39] Chakraborty T and Lee X 2019 A simplified urban-extent algorithm to characterize surface urban heat islands on a global scale and examine vegetation control on their spatiotemporal variability *Int. J. Appl. Earth Obs. Geoinf.* **74** 269–80
- [40] Swanson A, Holden Z A, Graham J, Warren D A, Noonan C and Landguth E 2022 Daily 1 km terrain resolving maps of surface fine particulate matter for the western United States 2003–2021 *Scientific Data* **9** 466
- [41] Childs M L, Li J, Wen J, Heft-Neal S, Driscoll A, Wang S, Gould C F, Qiu M, Burney J and Burke M 2022 Daily local-level estimates of ambient wildfire smoke PM<sub>2.5</sub> for the contiguous US *Environ. Sci. Technol.* **56** 13607–21
- [42] Derakhshan S, Emrich C T and Cutter S L 2022 Degree and direction of overlap between social vulnerability and community resilience measurements *PLoS One* **17** e0275975
- [43] Rygel L, O'sullivan D and Yarnal B 2006 A method for constructing a social vulnerability index: an application to hurricane storm surges in a developed country *Mitig. Adapt. Strateg. Glob. Change* **11** 741–64
- [44] MacManus K, Balk D, Engin H, McGranahan G and Inman R 2021 Estimating population and urban areas at risk of coastal hazards, 1990–2015: how data choices matter *Earth Syst. Sci. Data* **13** 5747–801
- [45] Raei E, Nikoo M R, AghaKouchak A, Mazdiyasi O and Sadegh M 2018 GHWR, a multi-method global heatwave and warm-spell record and toolbox *Sci. Data* **5** 1–15
- [46] Linkov I, Satterstrom F K, Kiker G, Batchelor C, Bridges T and Ferguson E 2006 From comparative risk assessment to multi-criteria decision analysis and adaptive management: recent developments and applications *Environ. Int.* **32** 1072–93
- [47] Lopez A D, Mathers C D, Ezzati M, Jamison D T and Murray C J 2006 Global and regional burden of disease and risk factors, 2001: systematic analysis of population health data *Lancet* **367** 1747–57
- [48] Broadbent A M, Declat-Barreto J, Kraysenoff E S, Harlan S L and Georgescu M 2022 Targeted implementation of cool roofs for equitable urban adaptation to extreme heat *Sci. Total Environ.* **811** 151326
- [49] Narain U, Margulis S and Essam T 2016 *Estimating Costs of Adaptation to Climate Change. International Climate Finance* (Routledge) pp 90–113
- [50] Nguyen T T, Bonetti J, Rogers K and Woodroffe C D 2016 Indicator-based assessment of climate-change impacts on coasts: a review of concepts, methodological approaches and vulnerability indices *Ocean Coast. Manage.* **123** 18–43
- [51] EPA 2024 Implementing the final rule to strengthen the national air quality health standard for particulate matter—clean air act permitting, air quality designations, and state planning requirements
- [52] Frank O, Tam C M and Rhee J 2021 Is it time to stop using statistical significance? *Aust. Prescr.* **44** 16–18
- [53] Mass C F, Ovens D, Conrick R and Saltenberger J 2021 The September 2020 wildfires over the Pacific Northwest *Weather Forecast.* **36** 1843–65
- [54] Chikamoto Y, Zhang W, Hipps L, Wang S S, Gillies R R and Bigalke S 2023 Interannual variability and trends of summertime PM<sub>2.5</sub>-based air quality in the Intermountain West *Environ. Res. Lett.* **18** 044032
- [55] Guo B, Zhang J, Meng X, Xu T and Song Y 2020 Long-term spatio-temporal precipitation variations in China with precipitation surface interpolated by ANUSPLIN *Sci. Rep.* **10** 81
- [56] Kim H, Yoo E-H, Senders A, Sergi C, Dodge H H, Bell S A and Hart K D 2024 Heat waves and adverse health events among dually eligible individuals 65 years and older *JAMA Health Forum* **5** e243884
- [57] Alizadeh M R, Abatzoglou J T, Adamowski J, Modaresi Rad A, AghaKouchak A, Pausata F S and Sadegh M 2023 Elevation-dependent intensification of fire danger in the western United States *Nat. Commun.* **14** 1773
- [58] Ummenhofer C C and Meehl G A 2017 Extreme weather and climate events with ecological relevance: a review *Phil. Trans. R. Soc. B* **372** 20160135
- [59] Torres-Gil F and Hofland B 2012 Vulnerable populations *Independent for Life* ed H Cisneros, M Dyer-Chamberlain and J Hickie (University of Texas Press) pp 221–32
- [60] Tong S, Prior J, McGregor G, Shi X and Kinney P 2021 Urban heat: an increasing threat to global health *bmj* **375** n2467
- [61] Achour N and Price A D 2010 Resilience strategies of healthcare facilities: present and future *Int. J. Disaster Resilience Built Environ.* **1** 264–76
- [62] Dong S, Esmalian A, Farahmand H and Mostafavi A 2020 An integrated physical-social analysis of disrupted access to critical facilities and community service-loss tolerance in urban flooding *Comput. Environ. Urban Syst.* **80** 101443
- [63] Toole M and Waldman R 1997 The public health aspects of complex emergencies and refugee situations *Annu. Rev. Public Health* **18** 283–312
- [64] Godde C M, Mason-D'Croz D, Mayberry D E, Thornton P K and Herrero M 2021 Impacts of climate change on the livestock food supply chain; a review of the evidence *Glob. Food Sec.* **28** 100488
- [65] Jaffe D A, O'Neill S M, Larkin N K, Holder A L, Peterson D L, Halofsky J E and Rappold A G 2020 Wildfire and prescribed burning impacts on air quality in the United States *J. Air Waste Manage. Assoc.* **70** 583–615
- [66] Ferguson L, Taylor J, Davies M, Shrubsole C, Symonds P and Dimitroulopoulou S 2020 Exposure to indoor air pollution across socio-economic groups in high-income countries: a scoping review of the literature and a modelling methodology *Environ. Int.* **143** 105748
- [67] McHale M R, Ludtke A S, Wetherbee G A, Burns D A, Nilles M A and Finkelstein J S 2021 Trends in precipitation chemistry across the U.S. 1985–2017: quantifying the benefits from 30 years of Clean Air Act amendment regulation *Atmos. Environ.* **247** 118219
- [68] Hobbie S E and Grimm N B 2020 Nature-based approaches to managing climate change impacts in cities *Phil. Trans. R. Soc. B* **375** 20190124
- [69] Pamukcu-Albers P, Ugolini F, La Rosa D, Grădinaru S R, Azevedo J C and Wu J 2021 Building green infrastructure to enhance urban resilience to climate change and pandemics *Landscape Ecol.* **36** 665–73
- [70] Pitman S D, Daniels C B and Ely M E 2015 Green infrastructure as life support: urban nature and climate change *Trans. R. Soc. South Aust.* **139** 97–112
- [71] Jay O, Capon A, Berry P, Broderick C, de Dear R, Havenith G, Honda Y, Kovats R S, Ma W and Malik A 2021 Reducing the health effects of hot weather and heat extremes: from personal cooling strategies to green cities *Lancet* **398** 709–24
- [72] Organization W H 2016 *Urban Green Spaces and Health* (World Health Organization. Regional Office for Europe)
- [73] Staddon C, Ward S, De Vito L, Zuniga-Teran A, Gerlak A K, Schoeman Y, Hart A and Booth G 2018 Contributions of green infrastructure to enhancing urban resilience *Environ. Syst. Decis.* **38** 330–8